Applied Mathematical Modelling 35 (2011) 2336–2347

Contents lists available at ScienceDirect

Applied Mathematical Modelling

journal homepage: www.elsevier.com/locate/apm

A posteriori error estimation and adaptive computation of conduction convection problems ☆

Yunzhang Zhang [a], Yanren Hou [a,*], Hongliang Zuo [b]

[a] School of Science, Xi'an Jiaotong University, Xi'an 710049, PR China
[b] College of Mathematics and Information Science, Henan Normal University, Xinxiang 453007, PR China

ARTICLE INFO

Article history:
Received 23 July 2009
Received in revised form 29 October 2010
Accepted 15 November 2010
Available online 25 November 2010

Keywords:
A posteriori analysis
Conduction convection problems
Mixed finite element
Adaptive finite element

ABSTRACT

In this paper, an adaptive finite element method is developed for stationary conduction convection problems. Using a mixed finite element formulation, residual type a posteriori error estimates are derived by means of the general framework of *R.* Verfürth. The effectiveness of the adaptive method is further demonstrated through two numerical examples. The first example is problem with known solution and the second example is a physical model of square cavity stationary flow.

1. Introduction

Let $\Omega \subset \mathbb{R}^2$ be a bounded and connected polygonal domain, with a Lipschitz continuous boundary Γ. We consider the stationary conduction–convection problems whose coupled equations governing viscous incompressible flow and heat transfer for the incompressible fluid are Boussinesq approximations to the stationary Navier–Stokes equations.

Find $u = (u_1, u_2)$, p and T such that

$$\begin{cases} -\nu\Delta u + (u\cdot\nabla)u + \nabla p = \lambda j T, & x \in \Omega, \\ \text{div}\quad u = 0, & x \in \Omega, \\ -\Delta T + \lambda u\cdot\nabla T = 0, & x \in \Omega, \\ u = 0, \quad T = T_0 & x \in \Gamma, \end{cases} \tag{1}$$

where $u = (u_1, u_2)$ represents the velocity vector, p the pressure, T the temperature, $\lambda > 0$ the Groshoff number, $j = (0, 1)$ the unit vector and $\nu > 0$ the viscosity.

Finding the numerical solution of conduction convection problems (1) is a difficult task. The reason is that the problem (1) not only contains the velocity vector field and the pressure field but also contains the temperature field. There are some works devoted to the development of efficient numerical schemes for these equations [1–5]. The non-stationary problem is considered, too [6–9].

Within the framework of finite element methods, generating optimal or near optimal meshes is a useful technique for increasing accuracy at a lower computational cost. A posteriori error estimates have been used with much success as a guid-

☆ Supported by NSF of China (Grant No. 10871156) and XJTU (Grant 2009xjtujc30).
* Corresponding author.
E-mail addresses: yzzmath@gmail.com (Y. Zhang), yrhou@mail.xjtu.edu.cn (Y. Hou), zuodke@yahoo.com (H. Zuo).

0307-904X/$ - see front matter © 2010 Elsevier Inc. All rights reserved.
doi:10.1016/j.apm.2010.11.033

ing tool in adaptively generating optimal or near optimal meshes and in adaptively computing solutions to problems with boundary layers (regions of rapid transition of the solution; see [10–13]). There are numerous works devoted to the development of the a posteriori analysis [14–19], for instance. R.Verfürth [14,17] has developed a general framework for a posteriori error estimates for nonlinear equations. In [18], Using the general framework, V.J. Ervin et al. derive the a posteriori error estimates for finite element approximations of viscoelastic fluid flows governed by differential constitutive laws of Giesekus and Oldroyd-B type. We also can find that the general framework has been used to derive a posteriori error analysis in [13,18,19]. In this paper, we will use the general framework of R.Verfürth [14,17] and derive a posteriori error estimates for finite element approximations of stationary conduction convection problems.

The present paper is organized as follows. In Section 2, we introduce some function spaces and recall some preliminary results. The general framework of R.Verfürth [14,17] is presented in Section 3. In Section 4, we cast the stationary conduction convection problems into the framework, that is, residual type a posteriori error estimates are derived for this problem. In Section 5, the effectiveness of the adaptive method is further demonstrated through two numerical examples. The first example is a known solution problem and the second example is a physical model of square cavity stationary flow. Conclusion is given in Section 6.

2. Functional setting and finite element approximation tools

In this section, we aim to describe some notations and results which will be frequently used in this paper. The Sobolev spaces and norms used in this context are standard [20]. We introduce the following Hilbert spaces.

$$\text{Velocity Space}: \quad M = H^1(\Omega)^2 = \left\{ v \in H^1(\Omega)^2 : v = 0 \text{ on } \partial\Omega \right\},$$

$$\text{Pressure Space}: \quad Q = L_0^2(\Omega) = \left\{ p \in L^2(\Omega), (p,1)_\Omega = 0 \right\},$$

$$\text{Temperature Space}: \quad W = H^1(\Omega), \quad W_0 = H_0^1(\Omega).$$

For ease of notation, we drop the domain from the norm and seminorm notations when the domain is obvious. We use the same notation for the corresponding norms of vector valued functions.

For problem (1), the following assumptions are recalled (see [6,20–22]).

($\mathbf{A}_1$) There exists a constant C_0 which only depends on Ω, such that

(i) $\|u\|_0 \leqslant C_0\|\nabla u\|_0,\ \|u\|_{0,4} \leqslant C_0\|\nabla u\|_0,\ \forall u \in H_0^1(\Omega)^2 (\text{or } H_0^1(\Omega))$,

(ii) $\|u\|_{0,4} \leqslant C_0\|u\|_1, \forall\ u \in H^1(\Omega)^2$,

(iii) $\|u\|_{0,4} \leqslant 2^{\frac{1}{2}}\|\nabla u\|_0^{\frac{1}{2}}\|u\|_0^{\frac{1}{2}},\ \forall u \in H_0^1(\Omega)^2 (\text{or } H_0^1(\Omega))$.

($\mathbf{A}_2$) Assuming $\partial\Omega \in C^{k,\alpha}(k \geqslant 0, \alpha > 0)$, then, for $\widetilde{T}_0 \in C^{k,\alpha}(\partial\Omega)$, there exists an extension $T_0 \in C_0^{k,\alpha}(\mathbb{R}^2)$, such that

$$\|T_0\|_{k,q} \leqslant \varepsilon, \quad k \geqslant 0, \quad 1 \leqslant q \leqslant \infty,$$

where ε is an arbitrary small positive constant number.

($\mathbf{A}_3$) $b(\cdot,\cdot,\cdot)$ and $\bar{b}(\cdot,\cdot,\cdot)$ have the following properties:

(i) For all $u \in M, v, w \in M (\text{or } T, \varphi \in H_0^1(\Omega))$, there holds

$$b(u,v,v) = 0, \quad b(u,v,w) = -b(u,w,v),$$
$$\bar{b}(u,T,T) = 0, \quad \bar{b}(u,T,\psi) = -\bar{b}(u,T,\psi),$$

where

$$b(u,v,w) = \frac{1}{2}\left[\int_\Omega \sum_{i,k=1}^{2} u_i \frac{\partial v_k}{\partial x_i} w_k dx - \sum_{i,k=1}^{2} u_i \frac{\partial w_k}{\partial x_i} v_k dx\right] \quad \forall u, v, w \in M,$$

$$\bar{b}(u,T,\psi) = \frac{1}{2}\left[\int_\Omega \sum_{i=1}^{2} u_i \frac{\partial T}{\partial x_i}\psi dx - \sum_{i}^{2} u_i \frac{\partial \psi}{\partial x_i} T dx\right], \quad \forall u \in M, \quad T, \psi \in W_0.$$

(ii) For all $u \in M$, $v \in M (\text{or } T \in W)$, $\forall w \in M (\text{or } \varphi \in W_0)$, there holds

$$|b(u,v,w)| \leqslant N\|\nabla u\|_0\|\nabla v\|_0\|\nabla w\|_0,$$
$$|\bar{b}(u,T,\varphi)| \leqslant \overline{N}\|\nabla u\|_0\|\nabla T\|_0\|\nabla \varphi\|_0,$$

where

$$N = \sup_{u,v,w} |b(u,v,w)|/(\|\nabla u\|_0\|\nabla v\|_0\|\nabla w\|_0),$$
$$\overline{N} = \sup_{u,T,\varphi} |\bar{b}(u,T,\varphi)|/(\|\nabla u\|_0\|\nabla T\|_0\|\nabla \varphi\|_0).$$

($\mathbf{A}_4$) Letting $A = 2\nu^{-1}\lambda(3C_0+1)\|T_0\|_1,\ B = 2\|\nabla T_0\|_0 + (2C_0^2\lambda)^{-1}\nu A$, then, there exist two positive constant δ_1, δ_2, such that

$$\nu^{-1}NA \leqslant 1-\delta_1, \quad 0<\delta_1\leqslant 1, \quad \delta_1^{-1}\nu^{-1}C_0^2B\overline{N} \leqslant 1-\delta_2, \quad 0<\delta_2\leqslant 1.$$

Theorem 2.1 [6]. *Under the assumption of* ($\mathbf{A}_1$) ∼ ($\mathbf{A}_4$), *then problem* (1) *has a unique solution* $(u, p, T) \in X \times M \times W$, and

$$\|\nabla u\|_0 \leqslant A, \quad \|\nabla T\|_0 \leqslant B.$$

Let $\Omega_h \subset \Omega$ *be the polygon region, such that mes* $(\Omega - \Omega_h) = 0$. *Let* $\Im_{h,j}(\Omega)$, $j \geqslant 1$, *be a the uniformly regular family of triangulations of* $\bar{\Omega}_h$, *indexed by a parameter* $h = \max_{K\in\Im_{h,j}(\Omega)}\{h_K; h_K = \mathrm{diam}(K)\}$, *which satisfies the following conditions:*

(1) Any two triangles in $\Im_{h,j}(\Omega)$ are either disjoint or share a complete smooth submanifold of their boundaries.
(2) The ratio $h_K/\varrho_K < \varrho$ is bounded from above independently of $K \in \Im_{h,j}(\Omega)$ and $h > 0$.

Here, ϱ_K and h_E denote the diameter of the largest ball inscribed into K and the diameter of an edge E of K, respectively. We note that condition (2) allows the use of locally refined meshes and it implies the ratio h_K/h_E, for all $K \in \Im_{h,j}(\Omega)$ and all edges E of K, is bounded from above and from below by constants which are independent of h, K and E.

For any $K \in \Im_{h,j}(\Omega)$, we denote by $\mathcal{E}(K)$ the set of its edges and by $\mathcal{E}_h = \cup_{K\in\Im_{h,j}(\Omega)}\mathcal{E}(K)$ the set of all edges of the triangulation. The set $\mathcal{E}_h$ may be decomposed as $\mathcal{E}_h = \mathcal{E}_{h,\Omega} \cup \mathcal{E}_{h,\Gamma}$, $\mathcal{E}_{h,\Omega} \cap \mathcal{E}_{h,\Gamma} = \phi$, where $\mathcal{E}_{h,\Gamma}$ denotes the set of all edges lying on Γ. For any $E \in \mathcal{E}_h$and any piecewise continuous function φ, we denote by $[\varphi]_E$ the jump of φ across E in a fixed direction. Here, φ is continued by 0 outside Ω and the direction is given by the exterior normal of Γ if $E \in \mathcal{E}_{h,\Gamma}$. Similarly, we define $\Im_h$ and $\Re_h$ as the collection of all the triangles and vertices, respectively, in the partition $\Im_{h,j}(\Omega)$.

For each triangle $K \in \Im_{h,j}(\Omega)$ and for each side $E \in \mathcal{E}_h$, we define:

$$\omega_K = \bigcup_{\{K':\mathcal{E}(K)\cap\mathcal{E}(K')\neq\phi\}} K', \quad \tilde{\omega}_K = \bigcup_{\{K':\partial K\cap\partial K'\neq\phi\}} K',$$
$$\omega_E = \bigcup_{\{K':E\in\mathcal{E}(K')\}} K', \quad \tilde{\omega}_E = \bigcup_{\{K':E\cap\partial K'\neq\phi\}} K'.$$

Let $W^{l,q}(\tilde{\omega}_K)$ and $W^{l,q}(\tilde{\omega}_E)$ be suitable Sobolev spaces defined on the extended neighborhoods of K and E, respectively. For $k \in \mathbb{N}$, we define

$$S_h^{k,-1} = \{\varphi : \Omega \to \mathbb{R} : \varphi|_K \in \mathbb{P}_k,\ \forall K \in \Im_{h,j}(\Omega)\}, \quad S_h^{k,0} = S_h^{k,-1} \cap C(\Omega),$$

where $\mathbb{P}_k$ is the space of polynomials of degree $\leqslant k$.

Let $\mathcal{S}_h : L^1(\Omega) \to S_h^{1,0}$ denote the interpolation operator of Clément [23]. Then, the following lemma holds.

Lemma 2.2 ([14,17]). *There exist two constants* c_1 *and* c_2, *depending only on the ratio* h_K/ϱ_K, *such that for* $K \in \Im_{h,j}(\Omega)$, $E \in \mathcal{E}_h$, *and* $1 \leqslant q \leqslant \infty$, *the following error estimates are valid:*

$$\|\varphi - \mathcal{S}_h\varphi\|_{k,q;K} \leqslant c_1 h_K^{l-k}\|\varphi\|_{l,q;\tilde{\omega}_K}, \quad 0\leqslant k\leqslant l\leqslant 2, \quad \varphi \in W^{l,q}(\tilde{\omega}_K),$$
$$\|\varphi - \mathcal{S}_h\varphi\|_{q;E} \leqslant c_2 h_E^{l-1/q}\|\varphi\|_{l,q;\tilde{\omega}_E}, \quad 1\leqslant l\leqslant 2, \quad \varphi \in W^{l,q}(\tilde{\omega}_E).$$

Let $V_K \subset L^\infty(K)$ and $V_E \subset L^\infty(E)$ denote fixed polynomial spaces defined on K and E respectively. For a simplex K with face E, let $P : L^\infty(E) \to L^\infty(K)$ be the continuation operator defined in [17], *and let* p *and* q *be two real numbers such that* $(1/p) + (1/q) = 1$, *then the following lemma holds.*

Lemma 2.3 ([14,17]). *There are constants* $c_1, \ldots, c_7$, *which only depend on the spaces* $V_{\tilde{K}}$ *and* $V_{\tilde{E}}$, *the functions* $\psi_{\tilde{K}}$ *and* $\psi_{\tilde{E}}$, *the number* p, *and the ratio* h_K/ϱ_K, *such that the following inequalities hold for all* $K \in \aleph_{h,j}$, $E \in \mathcal{E}_h$, $u \in V_K$, *and* $T \in V_E$:

$$c_1\|u\|_{0,p;K} \leqslant \sup_{v\in V_K}\frac{\int_K u\psi_K v}{\|v\|_{0,q;K}} \leqslant \|u\|_{0,p;K},$$

$$c_2\|T\|_{p;E} \leqslant \sup_{\tau\in V_E}\frac{\int_E u\psi_E\tau}{\|\tau\|_{q;E}} \leqslant \|T\|_{p;E},$$

$$c_3h_K^{-1}\|\psi_K u\|_{0,p;K} \leqslant \|\nabla(\psi_K u)\|_{0,q;K} \leqslant c_4h_K^{-1}\|\psi_K u\|_{0,p;K},$$

$$c_5h_K^{-1}\|\psi_E PT\|_{0,p;K} \leqslant \|\nabla(\psi_E PT)\|_{0,q;K} \leqslant c_6h_K^{-1}\|\psi_E PT\|_{0,p;K},$$

$$\|\psi_E PT\|_{0,p;K} \leqslant c_7h_K^{1/p}\|T\|_{p;E}.$$

In next section, we will present the abstract framework of R.Verfürth [14,17] for constructing a posteriori error estimates for nonlinear differential equations. We follow the notations used in R.Verfürth [14,17].

3. Abstract a posteriori error estimates

Let X and Y be two Banach spaces with the norms $\|\cdot\|_X$ and $\|\cdot\|_Y$, respectively. For any element $u \in X$ and any real number $R > 0$, define

$$B(u,R) = \{v \in X, \|u - v\|_X < R\}.$$

Let $\mathcal{Q}(X,Y)$ denote the Banach space of continuous linear maps from X to Y equipped with the operator norm $\|\cdot\|_{\mathcal{Q}(X,Y)^*}$. Denote by $\mathrm{Isom}(X,Y) \subset \mathcal{Q}(X,Y)$ the open subset of linear homeomorphisms of X onto Y. The dual space of Y, $Y^* = \mathcal{Q}(Y,\mathbb{R})$ and $\langle\cdot,\cdot\rangle$ represents the duality pairing between Y and $Y*$. Let $F \in C^1(X,Y*)$ be a continuously differentiable function. We denote the linearization of F about u_* by $DF(u_*)$, $Z = \|DF(u_*)\|_{\mathcal{Q}(X,Y)}$ and $\widehat{Z} = \|DF(u_*)^{-1}\|_{\mathcal{Q}(Y_D^*,X_D)}$.

Theorem 3.1 ([14,17]). *Let $u* \in X$ satisfy $F(u*) = 0$ and assume there exists (non-trivial) subspaces $X_D \subset X$, $Y_D^* \subset Y^*$ such that $DF(u_*) \in Isom(X_D, Y_D^*)$. In addition, assume that DF is Lipschitz continuous at $u*$, i.e., there is an $R* > 0$ such that*

$$\gamma = \sup_{u \in B(u_*,R_*)} \frac{\|DF(u) - DF(u_*)\|_{\mathcal{Q}(X,Y^*)}}{\|u - u_*\|_X} < \infty,$$

and let R be given by

$$R = min\left\{R_*, \gamma^{-1}\widehat{Z}^{-1}, 2\gamma^{-1}Z\right\}.$$

Then for any $u \in B(u*,R) \cap X_D$, we have the estimates

$$\frac{1}{2Z}\|F(u) - F(u_*)\|_{Y^*} \leqslant \|u - u_*\|_X, \tag{2}$$

and

$$\|u - u_*\|_X \leqslant 2\widehat{Z}\|F(u) - F(u_*)\|_{Y^*}. \tag{3}$$

Remark 3.2. From Remark 2.2 of [17], estimate (2) can be modified to obtain local estimates. Specifically, let $S = \mathrm{span}\{\psi_i\} \subset Y$, where support $(\psi_i) \subset \Lambda \subset \Omega$. Then,

$$\|F(u) - F(u^*)\|_{S^*} \leqslant 2Z\|(u - u_*)|_\Lambda\|_X. \tag{4}$$

Let $F_h \in C(X_h, Y_h^*)$ be an approximation of the function F. Denote the identity operator from Y to Y as Id_Y. Then, we have the following result.

Theorem 3.3 ([14,17]). *Let $u_h \in X_h$ be an approximate solution of the equation $F_h(u_h) = 0$, with $\|F_h(u_h)\|_{Y_h^*}$ "small". Assume that there is a restriction operator $\mathcal{R}_h \in \mathcal{Q}(Y, Y_h)$, a finite dimensional subspace $\widetilde{Y}_h = \mathrm{span}\{\psi_i\} \subset Y$, where support $(\mathrm{em}\ \psi_i) \subset \Lambda \subset \Omega$, and an approximation $\widetilde{F}_h : X_h \to \widetilde{Y}_h^*$ of F at u_h. Then,*

$$\begin{aligned}\|F(u_h)\|_{Y^*} \leqslant{}& \|(Id_Y - \mathcal{R}_h)\widetilde{F}_h(u_h)\|_{Y^*} + \|(Id_Y - \mathcal{R}_h)\left[F(u_h) - \widetilde{F}_h(u_h)\right]\|_{Y^*} + \|\mathcal{R}_h\|_{\mathcal{Q}(Y,Y_h)}\|F(u_h) - F_h(u_h)\|_{Y_h^*} \\ &+ \|\mathcal{R}_h\|_{\mathcal{Q}(Y,Y_h)}\|F_h(u_h)\|_{Y_h^*},\end{aligned} \tag{5}$$

and

$$\|\widetilde{F}_h(u_h)\|_{\widetilde{Y}_h^*} \leqslant \|F(u_h)\|_{\widetilde{Y}_h^*} + \|F(u_h) - \widetilde{F}_h(u_h)\|_{\widetilde{Y}_h^*}. \tag{6}$$

Remark 3.4. From Theorems 3.1 and 3.3, we get the basis for obtaining a residual based a posteriori error estimate.

Remark 3.5. In Theorem 3.3, operator $\mathcal{R}_h$ may be chosen as Clément [23] type interpolation operator. The space $\widetilde{Y}_h$ is the space spanned by a set of bubble functions constructed such that (6) holds. $\widetilde{F}_h(u_h)$ is a projection of $F_h(u_h)$ elementwise onto a suitable finite dimensional space.

Remark 3.6. Same as in[13,18,19], to apply the above framework to our problem, one relevant issue is how the various constants γ, Z, $\widehat{Z}$, and R depend on ν and λ. We note that obtaining a very precise dependence in general is very difficult. Some crude estimates can be obtained, for example, we can bound $Z = \|DF(u_*)\|_{\mathcal{Q}(X,Y^*)}$ by $\nu + 4N\nu^{-1}\lambda(3C_0 + 1)\|T_0\|_1 + 2\sqrt{2}+$

$\lambda C_0^2 + 2\lambda\overline{N}\nu^{-1}\lambda(3C_0+1)\|T_0\|_1 + 2\lambda\overline{N}\|\nabla T_0\|_0\overline{N}C_0^{-2}\lambda(3C_0+1)\|T_0\|_1$(see Remark 4.2). Similarly, one can estimate the Lipschitz constant γ(see Eq. (13)). For $\widehat{Z} = \|DF(u_*)^{-1}\|_{\mathcal{Q}(Y_D^*,X_D)}$, since $\widehat{Z}$ is a common multiplier of the right-hand side of (3), it is not for mesh redistribution, only for the computation of a reliable upperbound in order to check if a final stopping criterion is satisfied. Thus, we can approximate the multiplier $\|DF(u_*)^{-1}\|_{\mathcal{Q}(Y_D^*,X_D)}$ by $\|DF(u_h)^{-1}\|_{\mathcal{Q}(Y_h^*,X_h)}$, given an approximation solution $[u_h,p_h,T_h]$, where $X_h \subset X_D \subset X$ and $Y_h \subset Y \subset Y_D$ are appropriate finite element spaces. These estimates, however, are not sharp in general, and future studies are obviously needed to examine such dependence more carefully.

4. A Posteriori error estimation for conduction–convection problems

In order to cast problem (1) into the framework of §3, we set

$$X = M \times Q \times W, \quad Y = M \times Q \times W_0,$$
$$\|\cdot\|_X = \|\cdot\|_Y = \left\{\|\cdot\|_{1,2}^2 + \|\cdot\|_{0,2}^2 + \|\cdot\|_{1,2}^2\right\}^{1/2}.$$

We also define

$$\langle F([u,p,T]),[v,q,g]\rangle = \int_\Omega (\nu\nabla u\nabla v + (u\cdot\nabla)uv - p\nabla\cdot v + q\nabla\cdot u - \lambda jT\cdot v) + \int_\Omega(\nabla T\nabla g + \lambda u\cdot\nabla Tg), \quad \forall[v,q,g] \in [M,Q,W_0]. \tag{7}$$

We introduce finite element subspace $M_h \subset M$, $Q_h \subset Q$, $W_h \subset W$ as follows

$$M_h = \left\{v_h \in M \cap C^0(\bar\Omega)^2;\, v_h|_K \in P_k(K)^2,\, \forall K \in \Im_{hj}(\Omega)\right\},$$
$$Q_h = \left\{q_h \in Q \cap C^0(\bar\Omega);\, q_h|_K \in P_\ell(K),\, \forall K \in \Im_{hj}(\Omega)\right\},$$
$$W_h = \left\{g_h \in W \cap C^0(\bar\Omega);\, g_h|_K \in P_s(K),\, \forall K \in \Im_{hj}(\Omega)\right\},$$

where $P_\ell(K)$ is the space of piecewise polynomials of degree ℓ on K, $\ell \geqslant 1$, $k \geqslant 1$, $s \geqslant 1$ are three integers. We set $W_{0h} = W_h \cap H_0^1(\Omega)$ and assume (M_h,Q_h) satisfies the inf-sup (or LBB) condition. We set

$$X_h = M_h \times Q_h \times W_h, Y_h = M_h \times Q_h \times W_{0h},$$

and define

$$\langle F_h([u_h,p_h,T_h]),[v_h,q_h,g_h]\rangle = \langle F([u_h,p_h,T_h]),[v_h,q_h,g_h]\rangle. \tag{8}$$

In order to cast this discretization into the framework of §3, we define $\widetilde{F}_h$ in the same way as F. We define the restriction operator $\mathcal{R}_h : Y \to Y_h$ as

$$\mathcal{R}_h[u,p,T] = [\mathcal{S}_h u_1,\ldots,\mathcal{S}_h u_n, 0, \mathcal{S}_h T].$$

Let the polynomial degrees of the approximating spaces for u, p and T be k, ℓ, and s, respectively, then, the space $\widetilde{Y}_h$ is defined as

$$\widetilde{Y}_h = \mathrm{span}\Big\{[\psi_K v,0,0],[\underline{0},\psi_K q,0],[\underline{0},0,\psi_K g],[\psi_E Pw,0,0],[\underline{0},0,\psi_E Pr] : v \in [P_{m_1}(K)]^2, q \in [P_{k-1}(K)], g \in [P_{m_2}(K)], w \in [P_{m_3}(E)]^2, r \in [P_{m_4}(E)]\Big\},$$

where P is the continuation operator defined in [14,17], $\underline{0}$ is the zero vector and

$$m_1 = \max\{k,\ell-1,s\}, \quad m_2 = \max\{k,\ell-1,s\}, \quad m_3 = \max\{k-1,\ell,s-1\}, \quad m_4 = \max\{k-1,\ell,s-1\}.$$

For all $K \in \Im_{hj}(\Omega)$, we define local a posteriori error indicator by

$$\eta_K^2 = h_K^2\| -\nu\Delta u_h + (u_h\cdot\nabla)u_h + \nabla p_h - \lambda jT_h\|_{0,2;K}^2 + h_K^2\| - \triangle T_h + \lambda u_h\cdot\nabla T_h\|_{0,2;K}^2 + \|\nabla\cdot u_h\|_{0,2;K}^2 + h_E\|[\nu\partial_n u_h - p_h n]_E\|_{2,E}^2 + h_E\|[\partial_n T_h]_E\|_{0,2,E}^2. \tag{9}$$

Theorem 4.1. *Let $[u_*,p_*,T_*]$ be a weak solution of problem (1) which is regular in the sense of Theorem 3.1, and let $[u_h,p_h,T_h] \in [M_h,Q_h,W_h]$ be a solution of*

$$\langle F_h([u_h,p_h,T_h]),[v_h,q_h,g_h]\rangle = 0, \forall[v_h,q_h,g_h] \in [M_h,Q_h,W_h], \tag{10}$$

where F_h is given in Eq. (8), which is sufficiently close to $[u_*,p_*,T_*]$ in the sense of Theorem 3.1 and satisfies the assumptions of the Theorem 3.3. Then, for some constants c_8, c_9 the following a posteriori error estimates hold:

$$\left\{\|u_*-u_h\|_{1,2}^2 + \|p_*-p_h\|_{0,2}^2 + \|T_*-T_h\|_{1,2}^2\right\}^{1/2} \leqslant c_8\|DF(u_*,p_*,T_*)^{-1}\|_{\mathcal{Q}(Y_D^*,X_D)}\left\{\sum_{K\in\Im_{hj}(\Omega)}\eta_K^2\right\}^{1/2}, \tag{11}$$

and

$$\eta_K \leqslant c_9\|DF(u_*,p_*,T_*)\|_{\mathcal{Q}(X,Y^*)}\left\{\|u_*-u_h\|^2_{1,2;\omega_K}+\|p_*-p_h\|^2_{0,2;\omega_K}+\|T_*-T_h\|^2_{1,2;\omega_K}\right\}^{\frac{1}{2}}, \tag{12}$$

where η_K is defined by (9) and the constants c_8, c_9 only depend on the polynomial degrees of the spaces M_h, Q_h, W_h, domain Ω and on the ratio h_K/ϱ_K.

Proof. First, we establish the existence of the derivative of F and show that it is Lipschitz continuous in a neighborhood of $[u_*,p_*,T_*]$.

Let $DF_* \in \mathcal{Q}(X,Y^*)$ be defined by

$$\langle DF_*([u,p,T]),[v,q,g]\rangle = \int_\Omega(\nu\nabla u\nabla v+(u_*\cdot\nabla)uv+(u\cdot\nabla)u_*v-p\nabla\cdot v+q\nabla\cdot u-\lambda jT\cdot v)+\int_\Omega(\nabla T\nabla g+\lambda u_*\cdot\nabla Tg + \lambda u\cdot\nabla T_*g),\quad \forall[v,q,g]\in Y.$$

Now, using the continuous imbedding of H^1 in L^4, we have

$$\begin{aligned}&\langle F([u,p,T])-F([u_*,p_*,T_*])-DF_*([u-u_*,p-p_*,T-T_*]),[v,q,g]\rangle\\ &=\int_\Omega((u-u_*)\cdot\nabla)(u-u_*)v+\int_\Omega\lambda((u-u_*)\cdot\nabla)(T-T_*)g\\ &\leqslant N\|\nabla(u-u_*)\|_0^2\|\nabla v\|_0+\lambda\widetilde{N}\|\nabla(u-u_*)\|_0\|\nabla(T-T_*\|_0\|\nabla g\|_0\leqslant c\|[u,p,T]-[u_*,p_*,T_*]\|_X^2\|[v,q,g]\|_Y.\end{aligned}$$

We denote

$$G(F,DF)=F([u,p,T])-F([u_*,p_*,T_*])-DF_*([u-u_*,p-p_*,T-T_*]),$$

therefore

$$\lim_{[u,p,T]\to[u_*,p_*,T_*]}\frac{\|G(F,DF)\|_{\mathcal{Q}(X,Y^*)}}{\|[u,p,T]-[u_*,p_*,T_*]\|_X}=0.$$

It is said that F is differentiable about $[u_*,p_*,T_*]$.

Next, we check that the derivative DF is Lipschitz continuity. We let $DF_1(\cdot)$ denote the derivative at $[u_1,p_1,T_1]$. Then, for $[v,q,g]\in Y$, $[u,p,T]\in B([u_*,p_*,T_*],R*)$, we get

$$\begin{aligned}\langle DF_1([u,p,T])-DF_*([u,p,T]),[v,q,g]\rangle &= \int_\Omega[((u_1-u_*)\cdot\nabla)uv+(u\cdot\nabla)(u_1-u_*)v]\\ &\quad+\int_\Omega[\lambda((u_1-u_*)\cdot\nabla)Tg+\lambda(u\cdot\nabla)(T_1-T_*)g]\\ &\leqslant 2N\|\nabla(u_1-u_*)\|_0\|\nabla u\|_0\|\nabla v\|_0+\lambda\widetilde{N}\|\nabla(u_1-u_*)\|_0\|\nabla T\|_0\|\nabla g\|_0\\ &\quad+\lambda\widetilde{N}\|\nabla u\|_0\|\nabla(T_1-T_*)\|_0\|\nabla g\|_0\\ &\leqslant 2max\left\{N,\lambda\widetilde{N}\right\}\|[u_1,p_1,T_1]-[u_*,p_*,T_*]\|_X\|[u,p,T]\|_X\|[v,q,g]\|_Y,\end{aligned}$$

that is

$$\frac{\|DF_1([u,p,T])-DF_*([u,p,T])\|_{\mathcal{Q}(X,Y^*)}}{\|[u_1,p_1,T_1]-[u_*,p_*,T_*]\|_X}\leqslant 2max\left\{N,\lambda\widetilde{N}\right\}\|[u,p,T]\|_X\leqslant 2max\{N,\lambda\widetilde{N}\}(\|[u_*,p_*,T_*]\|_X+R_*)=\gamma. \tag{13}$$

We now construct the necessary bounds to the terms in (5) and (6). According to the definition of $\widetilde{F}_h$ and F, we can get

$$\left\|\widetilde{F}_h([u_h,p_h,T_h])-F([u_h,p_h,T_h])\right\|_{\widetilde{Y}_h^*}=0 \tag{14}$$

and

$$\left\|(Id_Y-\mathcal{R}_h)(\widetilde{F}_h([u_h,p_h,T_h])-F([u_h,p_h,T_h]))\right\|_{\widetilde{Y}_h^*}=0. \tag{15}$$

Based on the definition of $\widetilde{F}_h$, for all $[v,q,g]\in Y$, we have

$$\begin{aligned}\left\langle\widetilde{F}_h([u_h,p_h,T_h]),[v,q,g]\right\rangle &= \sum_{K\in\Im_{hj}(\Omega)}\left\{\int_K\{-\nu\triangle u_h+(u_h\cdot\nabla)u_h+\nabla p_h-\lambda jT_h\}v+\int_K q\nabla\cdot u_h\right\}+\sum_{K\in\Im_{hj}(\Omega)}\\ &\quad\times\int_K\{-\triangle T_h+\lambda u_h\cdot\nabla T_h\}g+\sum_{E\in\mathcal{E}_h}\int_E[\nu\partial_n u_h-p_hn]_Ev+\sum_{E\in\mathcal{E}_h}\int_E[\partial_nT_h]_Eg.\end{aligned} \tag{16}$$

For simple, we denote

$$
\begin{aligned}
R_1 &= -\nu\triangle u_h + (u_h\cdot\nabla)u_h + \nabla p_h - \lambda j T_h,\\
R_2 &= -\triangle T_h + \lambda u_h\cdot\nabla T_h,\\
R_3 &= \nabla\cdot u_h,\\
R_4 &= [\nu\partial_n u_h - p_h n]_E,\\
R_5 &= [\partial_n T_h]_E.
\end{aligned}
$$

From Lemmas 2.2 and 2.3, we have

$$
\begin{aligned}
\left\|(Id_Y-\mathcal{R}_h)\widetilde{F}_h([u_h,p_h,T_h])\right\|_{Y^*} = \sup_{\substack{[v,q,g]\in Y\\ \|[v,q,g]\|=1}}\Bigg|&\sum_{K\in\Im_{h,j}(\Omega)}\int_K\{R_1(v-\mathcal{S}_h v)+R_2(g-\mathcal{S}_h g)+qR_3\}\\
&+\sum_{E\in\mathcal{E}_h}\int_E\{R_4(v-\mathcal{S}_h v)+R_5(g-\mathcal{S}_h g)\}\Bigg| \leqslant c\left\{\sum_{K\in\Im_{h,j}(\Omega)}\eta_K^2\right\}^{1/2}. \qquad (17)
\end{aligned}
$$

By definition, we observe that

$$
\left\|(Id_Y-\mathcal{R}_h)[F([u_h,p_h,T_h])-\widetilde{F}_h([u_h,p_h,T_h])]\right\|_{Y^*}=0, \qquad (18)
$$

$$
\begin{aligned}
&\langle F([u_h,p_h,T_h])-F_h([u_h,p_h,T_h]),[v_h,q_h,g_h]\rangle=0,\\
&\|F([u_h,p_h,T_h])-F_h([u_h,p_h,T_h])\|_{Y_h^*}=0.
\end{aligned} \qquad (19)
$$

Combining (17)–(19) with (5) and (3), we can derive (11).

In order to prove inequality (6), we consider an arbitrary simplex $K\in\Im_{h,j}(\Omega)$ and an arbitrary face $E\in\mathcal{E}_h$ of K and define $\widetilde{Y}_h|_\omega$, $\omega\in\{K,\omega_E,\omega_K\}$, as in §2. The definition of space $\widetilde{Y}_h$ and Lemma 2.3 then yield the estimates

$$
\begin{aligned}
c_1c_4^{-1}h_K\|R_1\|_{0,2,K} &\leqslant \sup_{e\in[P_{m_1}(K)\setminus\{0\}]^2}\frac{\int_K R_1\psi_K e}{\|\nabla(\psi_K e)\|_{0,2,K}} = \sup_{e\in[P_{m_1}(K)\setminus\{0\}]^2}\frac{\left\langle\widetilde{F}_h([u_h,p_h,T_h]),[\psi_K e,0,0]\right\rangle}{\|\nabla(\psi_K e)\|_{0,2,K}}\\
&= \sup_{\substack{[v_b,q_b,g_b]\in\widetilde{Y}_h|_K\\ \|[v_b,q_b,g_b]\|_Y=1}}\left\langle\widetilde{F}_h([u_h,p_h,T_h]),[v_b,q_b,g_b]\right\rangle,
\end{aligned}
$$

$$
\begin{aligned}
c_1c_4^{-1}h_K\|R_2\|_{0,2,K} &\leqslant \sup_{f\in[P_{m_2}(K)\setminus\{0\}]}\frac{\int_K R_2\psi_K f}{\|\nabla(\psi_K f)\|_{0,2,K}} = \sup_{f\in[P_{m_2}(K)\setminus\{0\}]}\frac{\left\langle\widetilde{F}_h([u_h,p_h,T_h]),[0,0,\psi_K f]\right\rangle}{\|\nabla(\psi_K f)\|_{0,2,K}}\\
&= \sup_{\substack{[v_b,q_b,g_b]\in\widetilde{Y}_h|_K\\ \|[v_b,q_b,g_b]\|_Y=1}}\left\langle\widetilde{F}_h([u_h,p_h,T_h]),[v_b,q_b,g_b]\right\rangle,
\end{aligned}
$$

$$
\begin{aligned}
c_1\|R_3\|_{0,2,K} &\leqslant \sup_{w\in[P_{k-1}(K)\setminus\{0\}]}\frac{\int_K(\nabla\cdot u_h)\psi_K w}{\|w\|_{0,2,K}} = \sup_{w\in[P_{k-1}(K)\setminus\{0\}]}\frac{\left\langle\widetilde{F}_h([u_h,p_h,T_h]),[\underline{0},\psi_K w,0]\right\rangle}{\|\psi_K w\|_{0,2,K}}\\
&= \sup_{\substack{[v_b,q_b,g_b]\in\widetilde{Y}_h|_K\\ \|[v_b,q_b,g_b]\|_Y=1}}\left\langle\widetilde{F}_h([u_h,p_h,T_h]),[v_b,q_b,g_b]\right\rangle,
\end{aligned}
$$

$$
\begin{aligned}
c_2c_6^{-1}c_7^{-1}h_E^{1/2}\|R_4\|_{0,2,E} &\leqslant \sup_{\sigma\in[P_{m_3}(E)\setminus\{0\}]^2}c_2c_6^{-1}c_7^{-1}h_E^{1/2}\frac{\int_E R_2\psi_E P\sigma}{\|\sigma\|_{0,2,E}}\\
&= \sup_{\sigma\in[P_{m_3}(E)\setminus\{0\}]^2}c_2c_6^{-1}c_7^{-1}h_E^{1/2}\|\sigma\|_{0,2,E}^{-1}\cdot\left\{\langle\widetilde{F}_h([u_h,p_h,T_h]),[0,0,\psi_E P\sigma]\rangle-\int_{\omega_E}(R_1\psi_E P\sigma)\right\}\\
&\leqslant \sup_{\substack{[v_b,q_b,g_b]\in\widetilde{Y}_h|_K\\ \|[v_b,q_b,g_b]\|_Y=1}}\left\langle\widetilde{F}_h([u_h,p_h,T_h]),[v_b,q_b,g_b]\right\rangle+c_6^{-1}h_E\|R_1\|_{0,2;\omega_E}\\
&\leqslant c\sup_{\substack{[v_b,q_b,g_b]\in\widetilde{Y}_h|_K\\ \|[v_b,q_b,g_b]\|_Y=1}}\left\langle\widetilde{F}_h([u_h,p_h,T_h]),[v_b,q_b,g_b]\right\rangle,
\end{aligned}
$$

$$
\begin{aligned}
c_2c_6^{-1}c_7^{-1}h_E^{1/2}\|R_5\|_{0,2,E} &\leqslant \sup_{\mu\in[P_{m_4}(E)\setminus\{0\}]} c_2c_6^{-1}c_7^{-1}h_E^{1/2}\frac{\int_E R_5\psi_E P\mu}{\|\mu\|_{0,2,E}}\\
&= \sup_{\mu\in[P_{m_4}(E)\setminus\{0\}]} c_2c_6^{-1}c_7^{-1}h_E^{1/2}\|\mu\|_{0,2,E}^{-1}\cdot\left\{\langle\widetilde{F}_h([u_h,p_h,T_h]),[0,0,\psi_E P\mu]\rangle-\int_{\omega_E}(R_2\psi_E P\mu)\right\}\\
&\leqslant \sup_{\substack{[v_b,q_b,g_b]\in\widetilde{Y}_h|_K\\ \|[v_b,q_b,g_b]\|_Y=1}}\left\langle\widetilde{F}_h([u_h,p_h,T_h]),[v_b,q_b,g_b]\right\rangle+c_6^{-1}h_E\|R_2\|_{0,2;\omega_E}\\
&\leqslant c\sup_{\substack{[v_b,q_b,g_b]\in\widetilde{Y}_h|_K\\ \|[v_b,q_b,g_b]\|_Y=1}}\left\langle\widetilde{F}_h([u_h,p_h,T_h]),[v_b,q_b,g_b]\right\rangle.
\end{aligned}
$$

Combining all above inequalities with (9), we obtain

$$
\eta_K\leqslant c\sup_{\substack{[v_b,q_b,g_b]\in\widetilde{Y}_h|_K\\ \|[v_b,q_b,g_b]\|_Y=1}}\left\langle\widetilde{F}_h([u_h,p_h,T_h]),[v_b,q_b,g_b]\right\rangle. \tag{20}
$$

From the definition of $\widetilde{F}_h$, we get

$$
\left\|F([u_h,p_h,T_h])-\widetilde{F}_h([u_h,p_h,T_h])\right\|_{\widetilde{Y}_h^*}=0. \tag{21}
$$

Combining (20) and (21) with (4) and (6), we yield (12). □

Remark 4.2. The above theoretical analysis is used to guide us in the design of effective adaptive algorithms based on the a posteriori error estimator(9). A few comments are in order: as mentioned earlier, notice that the constants $c_8\|DF(u_*,p_*,T_*)^{-1}\|_{\mathcal{Q}(Y_D^*,X_D)}$ and $c_9\|DF(u_*,p_*,T_*)\|_{\mathcal{Q}(X,Y^*)}$ depend on ν and λ, since the constants $Z=\|DF(u_*,p_*,T_*)\|_{\mathcal{Q}(X,Y^*)}$ and $\widehat{Z}=\|DF(u_*,p_*,T_*)^{-1}\|_{\mathcal{Q}(Y_D^*,X_D)}$ have such a dependence. Some of these constants rely on a priori information and may not be easily computable; we thus cannot completely assure the reliability and efficiency of the a posteriori error bounds theoretically. Nevertheless, our numerical experiments demonstrate that a very effective adaptive algorithm can be implemented for conduction convection problems based on the a posteriori error estimator $\{\sum_K(\eta_K)^2\}^{1/2}$ as defined by (9). As mentioned earlier, we now present the crude estimate of $\|DF(u_*,p_*,T_*)\|_{\mathcal{Q}(X,Y^*)}$. In fact, by the definition of $DF(u_*,p_*,T_*)$, we can get

$$
\begin{aligned}
\|DF(u_*,p_*,T_*)\|_{\mathcal{Q}(X,Y^*)} &= \sup_{[u,p,T]\in X,[v,q,g]\in Y}\frac{\langle DF_*([u,p,T]),[v,q,g]\rangle}{\|[u,p,T]\|\|[v,q,g]\|}\leqslant \nu+2N\|\nabla u_*\|+2\sqrt{2}+\lambda C_0^2+\lambda\overline{N}\|\nabla u_*\|+\lambda\overline{N}\|\nabla T_*\|\\
&\leqslant \nu+2NA+2\sqrt{2}+\lambda C_0^2+\lambda\overline{N}A+\lambda\overline{N}B\leqslant \nu+4N\nu^{-1}\lambda(3C_0+1)\|T_0\|_1+2\sqrt{2}+\lambda C_0^2\\
&\quad+2\lambda\overline{N}\nu^{-1}\lambda(3C_0+1)\|T_0\|_1+2\lambda\overline{N}\|\nabla T_0\|_0+\overline{N}C_0^{-2}\lambda(3C_0+1)\|T_0\|_1.
\end{aligned}
$$

5. Numerical experiments

Our objectives here are mainly to illustrate the effectiveness of the adaptive methods. We present two numerical examples. The first example is a known solution problem and the second example deals with a benchmark problem [7]. The experiments are all implemented in the two-dimensional framework using public domain finite element software FreeFem++ [24]. To approximate the velocity and pressure, we use the Taylor–Hood approximation pair. The lagrange quadratic elements is used to approximate the temperature.

The adaptive strategy is carried out as follows.

First, set a tolerance $\eta*$; then we start from an initial triangulation $\Im_{h,0}(\Omega)$ and compute η.

- Step 1: If $\eta\leqslant\eta*$, stop. We obtain the final finite element solution. Otherwise, go to Step 2.
- Step 2: Compute η_K and η, generate a new mesh size h by the strategy presented in [24], and recompute η based on this new triangulation. Then go back to Step 1. For convenience of presentation, we introduce the following notation:
- N := number of elements for triangulation $\Im_{h,j}(\Omega)$;
- $I_{eff}:=\frac{\eta}{E_1}$ the effective index, i.e., the ratio between the related estimator and the true error. Here, $\eta^2=\sum_K(\eta_K)^2$, $E_1=\{E_1(u)^2+E_0(p)^2+E_1(T)^2\}^{1/2}$, $E_1(u)=\|u-u_h\|_{1,2}$, $E_0(p)=\|p-p_h\|_{0,2}$, $E_1(T)=\|T-T_h\|_{1,2}$.

Example 5.1. Known solution As in [18], $\Omega=[0,1]\times[0,1]$, and chosen functions are added to the right-hand side of (1) such that the exact solution of the problem is given by

$$T(x,y) = u_1(x,y) + u_2(x,y), u(x,y) = (u_1(x,y), u_2(x,y)),$$
$$u_1(x,y) = \left(1 - cos\left(\frac{2\pi(e^{r_1 x} - 1)}{e^{r_1} - 1}\right)\right) sin\left(\frac{2\pi(e^{r_2 y} - 1)}{e^{r_2} - 1}\right) \frac{r_2}{2\pi} \frac{e^{r_2 y}}{(e^{r_2} - 1)},$$
$$u_2(x,y) = -sin\left(\frac{2\pi(e^{r_1 x} - 1)}{e^{r_1} - 1}\right)\left(1 - cos\left(\frac{2\pi(e^{r_2 y} - 1)}{e^{r_2} - 1}\right)\right) \frac{r_1}{2\pi} \frac{e^{r_1 x}}{(e^{r_1} - 1)},$$
$$p(x,y) = r_1 r_2 sin\left(\frac{2\pi(e^{r_1 x} - 1)}{e^{r_1} - 1}\right) sin\left(\frac{2\pi(e^{r_2 y} - 1)}{e^{r_2} - 1}\right) \frac{e^{r_1 x} e^{r_2 y}}{(e^{r_1} - 1)(e^{r_2} - 1)},$$

where r_1 and r_2 are two strictly positive real parameters. The velocity field of this solution is similar to a counter clockwise vortex in a unit-box (see Fig. 1). Playing with the parameters r_1 and r_2, we can move the center of this vortex that has coordinates $x_0 = \frac{1}{r_1} log\left(\frac{e^{r_1}+1}{2}\right)$ and $y_0 = \frac{1}{r_2} log\left(\frac{e^{r_2}+1}{2}\right)$. Increasing r_1, the center goes rapidly towards the right-hand vertical side, whereas increasing r_2 it approaches the top edge. For the description of the above $(u_1(x,y), u_2(x,y), p(x,y))$, the readers also can see [16].

The numerical results for Example 5.1 are presented in Tables 1–4. Tables 1 and 2 present each grid used the total triangles N, approximate errors, the error indicator η and the effective index I_{eff} for Example 5.1 by using uniform procedures and by adaptive procedures, respectively. We notice from Table 1 that the effective index I_{eff} remain always in a neighborhood of 10.5, which confirms the reliability and efficiency of posteriori error indicator η. Comparing Tables 1 and 2, we observe that the errors of the adaptive procedures decrease much faster than those obtained by the quasi-uniform ones. For example, when the error around 0.0130001, we need 15842 Triangles by uniform procedures, while we only need 4423 Triangles by adaptive ones. This means we can save lots of work by the adaptive procedures than that by uniform procedures.

For physical coefficients ν and λ, we also report some numerical results in Tables 3 and 4. We find that the effective index I_{eff} decreases as ν or λ decreases, however, the effective index I_{eff} is less sensitive for λ than for ν. This question is currently under investigation.

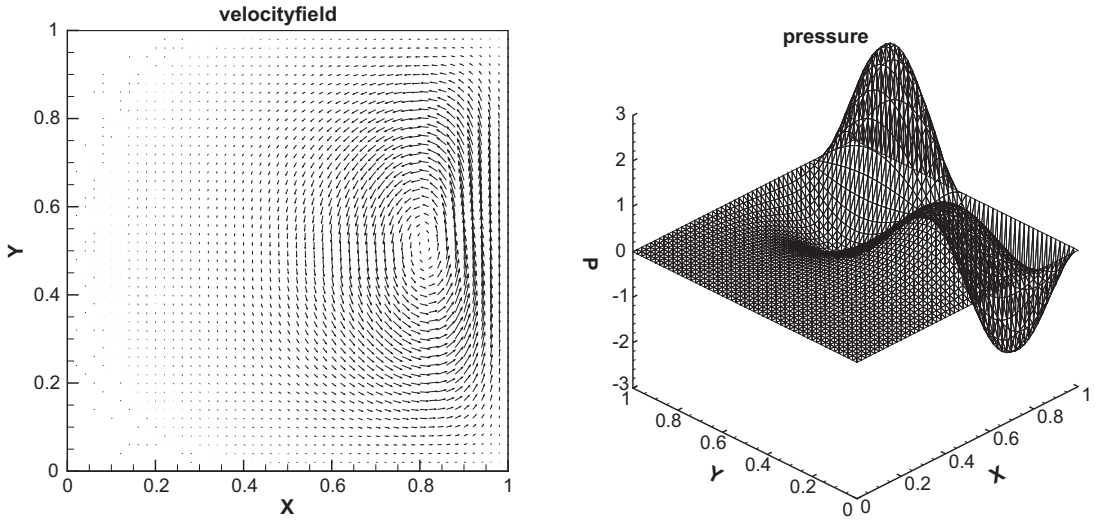

Fig. 1. Exact solution for $r_1 = 3.5$, $r_2 = 0.1$. (left): velocity field. (right): pressure.

Table 1
Uniform meshes for $\nu = 1.0$, $\lambda = 1.0$, $r_1 = 4.1$, $r_2 = 0.1$.

Mesh	N	$E_1(u)$	$E_0(p)$	$E_1(T)$	E_1	η	I_{eff}
12×12	288	0.41732	0.173035	0.376594	0.588149	4.99652	8.49533
16×16	512	0.240325	0.0763442	0.214324	0.330937	3.32426	10.045
24×24	1152	0.117942	0.0280296	0.106766	0.161539	1.71656	10.6263
32×32	2048	0.0694607	0.0149413	0.0633338	0.0951798	1.01273	10.6402
48×48	4608	0.031943	0.00642167	0.0292762	0.0438029	0.463137	10.5732
64×64	8192	0.0181863	0.00357096	0.016698	0.0249463	0.262625	10.5276
72×72	10368	0.0144165	0.0028126	0.0132432	0.019777	0.207903	10.5124
80×80	12800	0.0117048	0.00227299	0.0107559	0.016058	0.168618	10.5006
88×88	15488	0.0096902	0.00187528	0.00890696	0.0132948	0.139478	10.4912
89×89	15842	0.00947542	0.00183304	0.00870978	0.0130001	0.136374	10.4902
90×90	16200	0.00926768	0.00179221	0.00851905	0.0127152	0.133372	10.4892

Table 2
Adaptive meshes for $\nu = 1.0$, $\lambda = 1.0$, $r_1 = 4.1$, $r_2 = 0.1$.

N	$E_1(u)$	$E_0(p)$	$E_1(T)$	E_1	η	I_{eff}
172	0.496242	0.293	0.527071	0.780967	2.61738	3.35146
293	0.25333	0.119686	0.259643	0.381988	1.60124	4.19185
510	0.123429	0.0439571	0.123061	0.179752	0.986686	5.48914
1094	0.045364	0.0128941	0.045168	0.0653016	0.48127	7.36996
1808	0.0241433	0.00686228	0.0237789	0.0345749	0.290318	8.39679
2792	0.0147406	0.00437071	0.0145405	0.0211616	0.187505	8.86062
4423	0.00910426	0.00251417	0.00902693	0.013065	0.119078	9.11426
5726	0.00712507	0.00202163	0.0070154	0.0102014	0.0949947	9.31189
7258	0.00552339	0.00170527	0.00539269	0.0079055	0.0745884	9.43501
9520	0.00408493	0.00118323	0.00401302	0.00584731	0.0556845	9.5231
11885	0.00337291	0.00096654	0.00338277	0.00487379	0.0462988	9.49953
14121	0.00284108	0.000890163	0.00286308	0.00413054	0.0388237	9.39918
17495	0.0020751	0.000583912	0.00207008	0.00298868	0.0276867	9.26383

Table 3
$\nu = 1$, $h = 1/32$, $r_1 = 0.1$, $r_2 = 0.1$.

λ	$E_1(u)$	$E_0(p)$	$E_1(T)$	E_1	η	I_{eff}
10	0.00408709	0.00165679	0.0021204	0.0048934	0.0516914	10.5635
8	0.00408684	0.00164672	0.00209684	0.00487962	0.0511647	10.4854
6	0.00408689	0.00166502	0.00207887	0.00487819	0.0507646	10.4065
4	0.0040867	0.00163904	0.00206517	0.00486338	0.0504844	10.3805
2	0.00408684	0.00164652	0.00205755	0.00486279	0.0503182	10.3476
1	0.00408668	0.00163804	0.00205435	0.00485845	0.050263	10.3455

Table 4
$\lambda = 1$, $h = 1/32$, $r_1 = 0.1$, $r_2 = 0.1$.

ν	$E_1(u)$	$E_0(p)$	$E_1(T)$	E_1	η	I_{eff}
2	0.00408075	0.00163845	0.00205435	0.0048536	0.0818078	16.8551
1.5	0.00408229	0.00163821	0.00205435	0.00485481	0.0652859	13.4477
1	0.00408668	0.00163804	0.00205435	0.00485845	0.050263	10.3455
0.5	0.00411031	0.00163794	0.00205435	0.0048783	0.0385358	7.89943
0.2	0.00427205	0.00163791	0.00205435	0.00501533	0.0345641	6.89169
0.1	0.00480547	0.00163791	0.00205435	0.00547683	0.0340245	6.21244

Example 5.2. Square cavity stationary flow The second example is a physical model of square cavity stationary flow [7]. The side length of the square cavity and the boundary conditions are given in Fig. 2. From Fig. 1, we can see that $T = 0$ on left and lower boundaries, $\frac{\partial T}{\partial n} = 0$ on upper boundary, and $T = 4y(1 - y)$ on right boundary of the cavity. In this example, we set $\lambda = 1$ and $\nu = 0.1$.

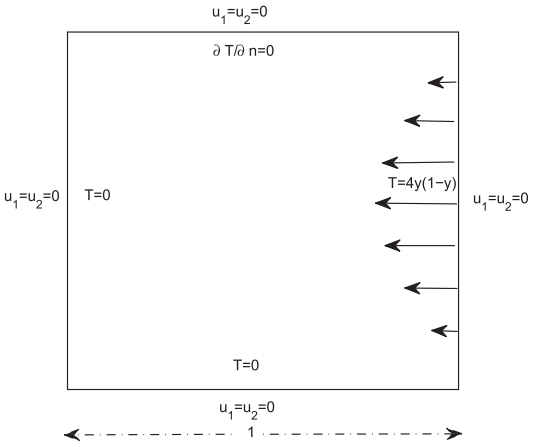

Fig. 2. Physics model of the cavity flows.

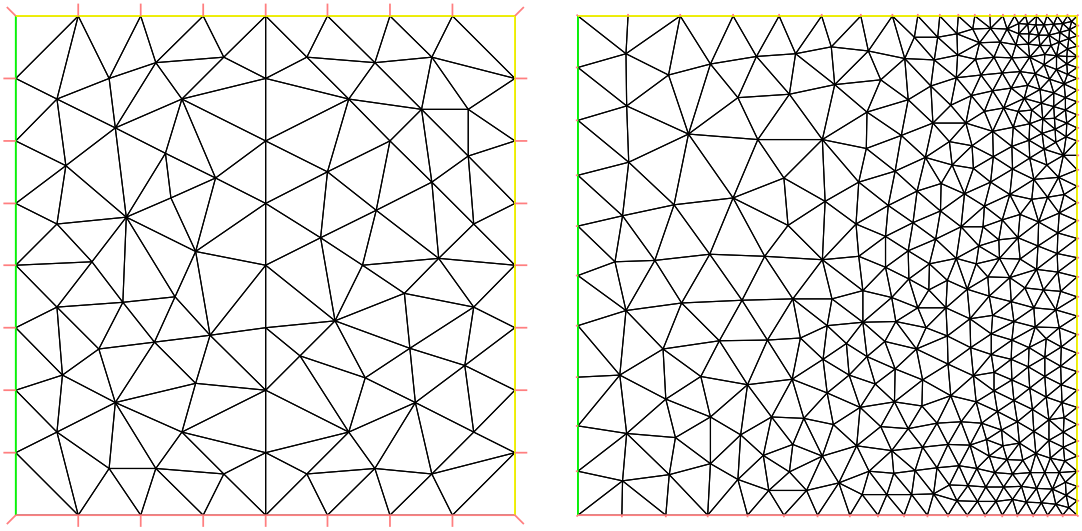

Fig. 3. Initialization mesh (left). The first adaptation mesh using the error indicator (right).

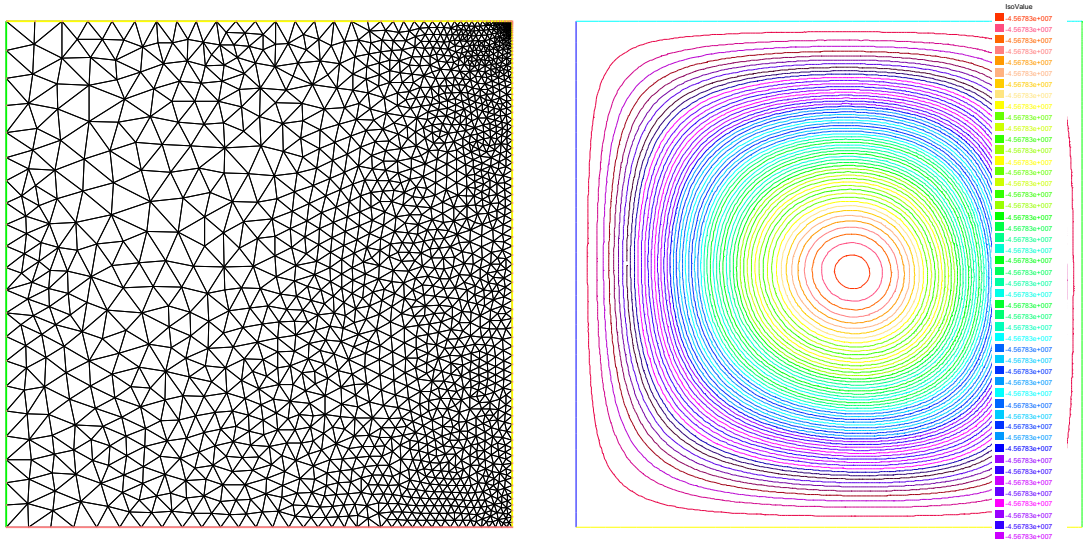

Fig. 4. The third adaptation mesh using the error indicator (left). The streamlines of velocity numerical solutions after three levels of adaptation mesh refinement (right).

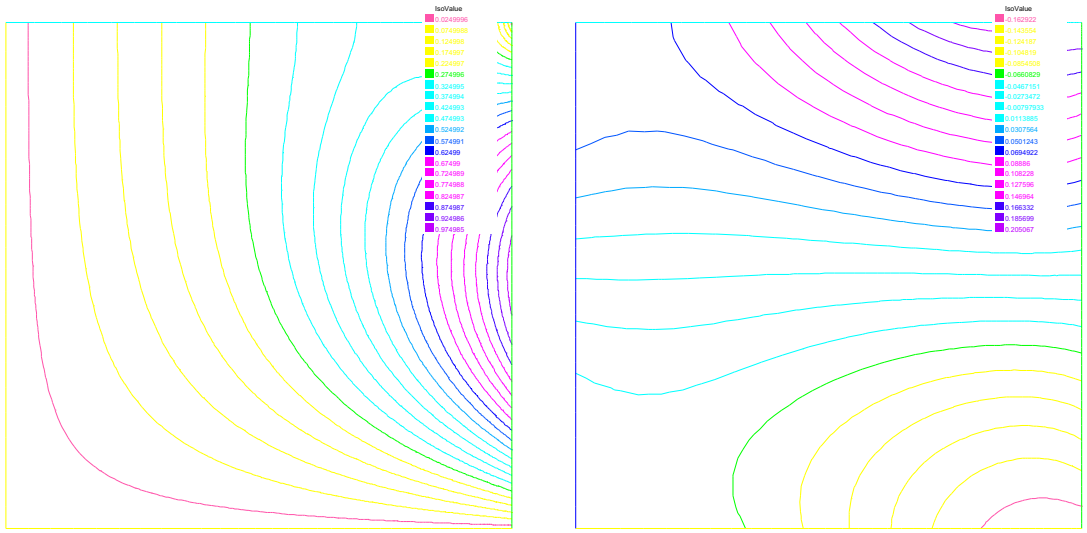

Fig. 5. Numerical isotherm of temperature solution after three levels of adaptation mesh refinement (left). Numerical isobar of pressure solution after three levels of adaptation mesh refinement (right).

We first give initialization mesh (the left of Fig. 3). Then we generate adaptive meshes based on the a posteriori error estimate (9). The right of Fig. 3 and the left of Fig. 4 are one and three levels of adaptive meshes, respectively. From these adaptively generated meshes, we see that our method is able to recognize the singularities and the regions with high gradients of the solutions. After three levels of adaptive meshes refinement, we present the numerical solution of (u_h, T_h, p_h). The right of Fig. 4 is the streamlines of velocity numerical solutions. The left and right of Fig. 5 are numerical isotherm and numerical isobar, respectively.

6. Conclusion

In this paper, based on mixed finite element formulation and the general framework of R.Verfürth [14,17], residual type a posteriori error estimates are derived for the stationary conduction convection problems. The effectiveness of the adaptive method is further demonstrated through two numerical examples. The first example is problem with known solution and the second example is a physical model of square cavity stationary flow. Precise information on the dependence of the constants in the a posteriori error estimates on the coefficients ν and λ is currently under investigation.

Acknowledgements

The authors thank the anonymous referee and editors for their valuable comments and suggestions which helped to greatly improve the paper.

References

[1] Z. Luo, X. Lu, A least squares Galerkin/Petrov mixed finite element method for the stationary conduction–convection problems, Math. Numer. Sin. 25 (2003) 31–244.
[2] Z. Luo, X. Lu, A nonlinear Galerkin/Petrov least squares mixed finite element method for the stationary conduction–convection problems, Math. Numer. Sin. 25 (2003) 447–462.
[3] M.S. Mesquita, M.J.S. de Lemos, Optimal multigrid solutions of two-dimensional convection–conduction problems, Appl. Math. Comput. 152 (2004) 725–742.
[4] Q.W. Wang, M. Yang, W.Q. Tao, Natural convection in a square enclosure with an internal isolated vertical plate, Warme-Stoffubertrag 29 (1994) 161–169.
[5] M. Yang, W.Q. Tao, Q.W. Wang, S.S. Lue, On identical problems of natural convection in enclosure and applications of the identity character, J. Thermal Sci. 2 (1993) 116–125.
[6] Z. Luo, Mixed Finite Element Foundation and its Application, Science Press, Beijing, 2006. in Chinese.
[7] Z. Luo, J. Chen, I.M. Navon, J. Zhu, An optimizing reduced PLSMFE formulation for non-stationary conduction–convection problems, Int. J. Numer. Meth. Fluids 60 (2009) 409–436.
[8] Z. Luo, L. Wang, Nonlinear Galerkin mixed element methods for the non stationary conduction–convection problems (I): the continuous-time case, C. J. Numer. Math. Appl. 20 (4) (1998) 71–94.
[9] J.N. Reddy, D.K. Gartling, The Finite Element Method in Heat Transfer and Fluid Dynamics, CRC Pess, Washington, 2001.
[10] K. Eriksson, C. Johnson, Adaptive streamline diffusion finite element methods for stationary convection–diffusion problems, Math. Comput. 60 (1993) 167–188.
[11] H. Zheng, Y. Hou, F. Shi, Adaptive variational multiscale methods for incompressible flow based on two local Gauss integrations, J. Comput. Phys. 229 (2010) 7030–7041.
[12] H. Zheng, Y. Hou, F. Shi, A posteriori error estimates of stabilization of low-order mixed finite elements for incompressible flow, SIAM J. Sci. Comp. 32 (2010) 1346–1361.
[13] V.J. Ervin, W.J. Layton, J.M. Maubach, An adaptive defect correction method for viscous incompressible flow problems, SIAM J. Numer. Anal. 37 (2000) 1165–1185.
[14] R. Verfürth, A Review of a Posteriori Error Estimation and Adaptive Mesh-Refinement Techniques, Wiley Teubner, 1996.
[15] M. Ainsworth, J.T. Oden, A Posteriori Error Estimation in Finite Element Analysis, Wiley Interscience, New York, 2000.
[16] S. Berrone, Adaptive discretization of stationary and incompressible Navier–Stokes equations by stabilized finite element methods, comput, Meth. Appl. Mech. Eng. 190 (2001) 4435–4455.
[17] R. Verfürth, A Posteriori Error Estimates for Nonlinear Problems, Finite Elem. Discretizations Elliptic Equ. Math. Comput. 62 (1994) 445–475.
[18] V.J. Ervin, Louis N. Ntasin, A posteriori error estimation and adaptive computation of viscoelastic fluid flows, Numer. Methods Partial Differential Eq. 21 (2005) 297–322.
[19] Q. Du, J. Zhang, Adaptive finite element method for a phase field bending elasticity model of vesicle membrane deformations, SIAM J. Sci. Comput. 30 (3) (2008) 1634–1657.
[20] R. Adams, Sobolev space, Pure and Applied Mathematics, vol. 65, Academic press, New York, 1975.
[21] Y. He, J. Li, Convergence of three iterative methods based on the finite element discretization for the stationary Navier–Stokes equations, Comput. Methods Appl. Mech. Eng. 198 (2009) 1351–1359.
[22] R. Temam, Navier–Stokes equation: Theory and Numerical Analysis, Third ed., North-Holland, Amsterdam, New York, Oxford, 1984.
[23] P. Clément, Approximation by finite elements using local regularization, RAIRO Anal. Numér. 2 (1975) 77–84.
[24] F.Hecht, O.Pironneau, A. Le Hyaric, K. Ohtsuka, FreeFem++, 2008. <http://www.freefem.org/ff>++.